2013 IEEE/RSJ International Conference on
Intelligent Robots and Systems (IROS)
November 3-7, 2013. Tokyo, Japan

Stability and Performance of the Compliance Controller of the Quadruped Robot HyQ

Thiago Boaventura[1], Gustavo A. Medrano-Cerda[1],
Claudio Semini[1], Jonas Buchli[2], Darwin G. Caldwell[1]

Abstract— **A legged robot has to deal with environmental contacts every time it takes a step. To properly handle these interactions, it is desirable to be able to set the foot compliance. For an actively-compliant legged robot, in order to ensure a stable contact with the environment the robot leg has to be passive at the contact point. In this work, we asses some passivity and stability issues of the actively-compliant leg of the quadruped robot HyQ, which employs a high-performance cascade compliance controller. We demonstrate that both the nested torque loop performance as well as the actuator bandwidth have a strong influence in the range of virtual impedances that can be passively rendered by the robot leg. Based on the stability analyses and experimental results, we propose a procedure for designing cascade compliance controllers. Furthermore, we experimentally demonstrate that the HyQ's actively-compliant leg is able to reproduce the compliant behavior presented by an identical but passively-compliant version of the same leg.**

I. Introduction

More and more robots have to interact with the environment around them, with humans, tools or other objects. Physical contacts are inherent to robotics applications such as assembly, service duties, and legged locomotion. To properly handle these physical contacts, it is essential to be able to control the interaction forces, or more generically speaking, to control the robot's compliance.

Compliance at the end-effector (or contact point) can be achieved in two ways: *passively* or *actively* [1], [2]. *Passive compliance* is obtained through hardware and can be attributed to physical elements such as the limited stiffness of the robot's links, the compliance of the actuator transmission (e.g. springs, gearboxes, harmonic drives, hydraulic oil, air, etc), and the softness of the robot "skin" (e.g. a layer of rubber around the end-effector). On the other hand, *active compliance* is achieved via the control of the joint torques, regardless of additional passive elements.

There are many ways of actively controlling the compliance at the end-effector (e.g. impedance control [3], operational space control [4], and virtual model control [5]). However, their practical implementation has been challenging because of the technological limitations such as computing power, communication technologies, sensors, and electronics integration. Some of these factors used to cause stability problems and made impossible to increase the force gains, strongly limiting the closed-loop force control bandwidth [6]. The sluggish performance obtained restricted for many years the use of active compliance to applications with very slow dynamics [7].

One solution to overcome the stability issues in force control has been found in introducing springs in series with the actuator [8]. Besides reducing the transmission stiffness and making the force control problem easier, the spring in series elastic actuators (SEAs) has also three other important functions: (a) to protect the actuator (or gearbox) from damage due to impact forces, (b) to store energy, and (c) to be backdrivable and possibly safer during human-robot interaction, for instance. The design of SEAs requires a trade-off between robustness and task performance. To choose the most appropriate spring stiffness is not a trivial task and it can seriously limit the robot versatility. In order to avoid this trade-off, several variable stiffness actuators (VSAs) have been recently proposed [9], [10], [11]. However, even though VSA is a promising solution for compliant robots, aspects such as weight, volume, complexity, and velocity saturation still limit its use in highly-dynamic robots. Moreover, since low joint stiffness reduces the robot controllability and also position tracking capabilities, commonly VSAs operate in a higher stiffness configuration. In these cases, the safety hallmark of passive compliance is basically lost.

With the technological development of the last two decades, active compliance for highly-dynamic applications became feasible [12], [13]. However, the current limitations for the use of active compliance in highly-dynamic legged robots are still not totally clear, especially in the presence of impacts or other high-frequency disturbances. Several aspects are not discussed in the literature, such as the maximum leg stiffness and damping which ensure a stable contact with the environment. This dynamic range of achievable virtual impedances is often called *Z-width* (where Z stands for impedance). Although the Z-width for virtual environments has been intensively investigated for haptics devices [14], [15], to the best of our knowledge there are no studies on the achievable range of impedances for virtual components in legged robots and neither studies that consider the impact of a nested torque closed loop in such range.

In this contribution, we discuss and clarify these and other important issues which can limit the use of active compliance in legged robots. This paper builds upon the already presented works [12] and [16], which focused in the design, implementation, and application of a high-

[1] T.Boaventura, G.A. Medrano-Cerda, C. Semini and D.G. Caldwell are with the Department of Advanced Robotics, Istituto Italiano di Tecnologia (IIT). tboventura@ethz.ch, <gustavo.cerda>, <claudio.semini>, <darwin.caldwell>@iit.it.

[2] J. Buchli is with the Agile & Dexterous Robotics Lab, ETH Zurich. buchlij@ethz.ch

performance torque controller to reach active compliance with the quadruped robot HyQ [17]. The main contributions of this work are: for the first time the concept of *Z-width* [18], which is well-known in haptics, is extended to legged robots; it demonstrates the influence of the torque control performance and actuator bandwidth in the Z-width; it gets insights from the passivity and performance analyses to propose a simple procedure for designing compliance controllers; it *experimentally* shows, to the best of our knowledge for the first time, that a completely actively-compliant leg can achieve the same compliance behavior as a passive leg configuration.

The paper is structured as follows: in Sec. II we present the actively-compliant leg of HyQ and how we implemented virtual elements on it. Next, in Sec. III we show the achievable impedance range for the HyQ virtual components and also how the torque loop gain and the actuator bandwidth influence this range. The experimental results are described in Sec. IV, where we demonstrate the importance of a high-bandwidth closed-loop torque control to achieve dynamic compliant behaviors without any springs on it. In Sec. V we propose a procedure for designing compliance controllers and we draw a comparison between active and passive compliance, discussing the results obtained. Then, in Sec. VI we address the conclusions and discuss future directions.

II. Active Compliance

In nature animals are constantly using muscle power for achieving adjustable compliance. Legged animals, for example, adapt their leg muscle stiffness according to the performed motion and terrain [19]. The capability to change between different stiffness profiles permits to choose the most suitable compliance characteristic for a certain situation. Being able to mimic this adaptive capability is a big step towards truly versatile robots and the main motivation behind the use of active compliance.

This section presents briefly how we implemented active compliance in the HyQ robot leg. HyQ is a fully torque-controlled robot, with a mix of hydraulic and electric actuation. The HyQ compliance controller uses a cascade control architecture, as depicted in Fig. 1. It consists in an outer compliance loop that manipulates the reference input of an inner torque control loop. The high-performance of the inner torque controller, obtained through low-level model-based techniques [12], [20], was essential for being able to successfully achieve compliance through software, without any real spring on it.

An intuitive and easy way of setting a desired compliance profile to a robot is through virtual model control [5]. In this framework, virtual elements that have physical counterparts, for example mechanical spring, damper, and so on, are placed at points of interest within the reference frames of the robot. Once the placement is done, we can define the Jacobian matrix that relates the virtual components velocities to the joints velocities. Then, through the Jacobian transpose the interaction forces between these components and the robot generate the desired joint torques at the actuators. As we show in Sec. IV-A, the effectiveness of this procedure is highly dependent on the torque tracking capabilities of the system. Considering the closed-loop systems is stable, the higher the performance of the torque control the closer we are to realize the desired behavior of the virtual elements.

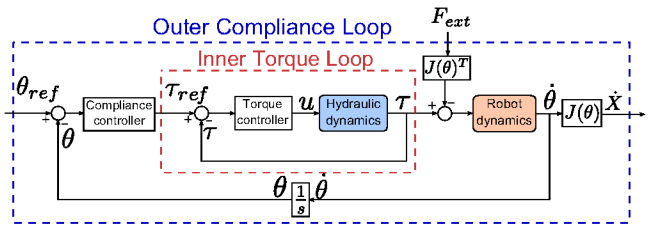

Fig. 1. Block diagram of the HyQ compliance control architecture. The external force vector F_{ext}, which is translated to joint space through the end-effector Jacobian matrix $J(\theta)$, acts as a perturbation into the system. The end-effector admittance matrix Y relates the the external forces F_{ext} with the end-effector velocities $\dot{X}$.

For making the HyQ robot actively-compliant, we use a spring-damper between the hip and the foot, as depicted in Fig. 2(a). The desired force F created by these virtual components can be linear or nonlinear with respect to the stiffness K, damping B, and virtual prismatic leg length l. The use of the virtual prismatic leg is also a simple way of actively implementing the well-known spring loaded inverted pendulum (SLIP) model [21], which is an useful abstraction that describes the spring-like behavior found in human and animal running and walking [22].

III. Passivity of the HyQ Leg

It is well-known that, for a linear time invariant system, a necessary and sufficient condition to ensure a stable contact with any passive environment is that the system has also to be passive at the interaction port [23]. For a nonlinear system, this is also a sufficient condition to guarantee a stable contact with a passive environment [24]. Thus, since most terrain surfaces are passive, it would be very convenient for a legged robot to make sure the leg behaves passively at the foot. In this section, we will analyze the main factors that influence the passivity of the HyQ's actively-compliant leg.

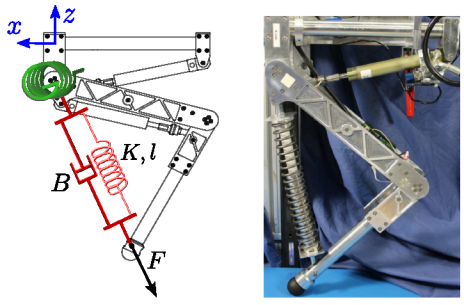

(a) (b)

Fig. 2. (a): HyQ virtual elements: a spring-damper connects the hip to the foot (red elements), creating a *prismatic virtual leg*. In the hip joint, a simple joint-space position PD control can be seen as a rotational spring-damper (green element). (b): HyQ leg with a real spring-damper in place of the knee hydraulic actuator. These virtual and real elements will be compared in Sec. IV-B.

When compliance is reached by assembling a real physical spring or damper onto the leg, it is certain that this component is intrinsically passive. In other words, it cannot provide additional energy to the system. However, when compliance is obtained actively, the compliant behavior is emulated by a controlled actuator, which can inject energy into the system.

The mechanical driving-point impedance (denoted Z) is defined as the dynamic operator that determines an output force from an input velocity at the interaction port. The admittance Y, on the other hand, is defined as the inverse of the impedance Z, that is, it determines the output velocity given an input force [25]. For a multiple input-multiple output (MIMO) system, as the HyQ leg, the admittance $Y(s)$ is a matrix which groups individual transfer functions that are represented in the Cartesian orientations x and z (see Fig. 2(a)). It can be defined as:

$$\dot{X}(s) = Y(s)\ F_{ext}(s)$$

$$\begin{bmatrix}\dot{X}_x(s)\\ \dot{X}_z(s)\end{bmatrix} = \begin{bmatrix}Y_{xx}(s)\ Y_{xz}(s)\\ Y_{zx}(s)\ Y_{zz}(s)\end{bmatrix}\begin{bmatrix}F_{ext_x}(s)\\ F_{ext_z}(s)\end{bmatrix} \quad (1)$$

where,

$\dot{X}$: velocity vector at the end-effector

F_{ext}: external forces vector applied at the end-effector

The admittance transfer functions in $Y(s)$ can be obtained through the block diagram shown in Fig. 1, which uses the end-effector Jacobian matrix $J(\theta)$ to relate joint and task space variables.

Necessary and sufficient conditions for passivity of a linear time invariant multi-port system are well-known in the literature [26]. Considering (1), $Y(s)$ is passive if and only if:

1. $Y(s)$ has no poles in right-half plane $\Re(s) > 0$;
2. $Y(s) + Y^*(s)$ is positive semi-definite in $\Re(s) > 0$;

where $Y^*(s)$ is the conjugate transpose of $Y(s)$.

When $Y(s)$ has no poles in $\Re(s) \geq 0$, then condition 2 can be simplified to:

2a. The matrix $Y(j\omega) + Y^*(j\omega)$ is positive semi-definite for all real ω.

In this case, it is possible to evaluate condition $2a$ by computing the minimum eigenvalue of $Y(j\omega) + Y^*(j\omega)$ as a function of ω, and by checking that this is not negative.

For sampled data control systems, [27] has suggested an approximate method based on computing the corresponding discrete time transfer function matrix $Y(z)$, assuming that the port of interaction is also sampled. The phase of all the entries in $Y(z)$ is computed and corrected by adding $\omega T_s/2$ rad to each term, where T_s is the sampling time interval. After this correction, the modified matrix and its conjugate transpose are added and the smallest eigenvalue computed. To guarantee passivity, this eigenvalue cannot be negative and $Y(z)$ should not have poles outside the unit circle.

A. Torque control & Z-width

In haptics, the range of position gains that keep the end-effector (the leg, in our case) passive is called Z-width [18]. In other words, Z-width is the range of achievable virtual impedances, and it defines the combinations of stiffness and damping that can be passively rendered by a certain mechanism.

However, to the best of our knowledge, the results presented in the literature involve haptics devices that are, in general, simple and often composed of only one DOF. Also, in these studies a force/torque control loop was not employed and the devices were only position controlled [14]. Therefore, some of the results present in the literature about the Z-width might not be directly applicable to more complex systems with different control architectures as the HyQ leg. Thus, in this section we aim to clarify the importance of the torque loop in the HyQ leg passivity as well as to show that also the actuator bandwidth plays an important role in the Z-width. The results presented in here can also be applied to other systems besides legged robots.

The results obtained in [14] suggest that the intrinsic system capability of dissipating energy, represented by the viscous friction, is the most important parameter for determining the size of the Z-width. Practically, the bigger the friction, the bigger the range of achievable impedances. In other words, you cannot inject more energy than your system can naturally dissipate. And that is an advantage of hydraulic actuators, which usually have intrinsically high viscous friction for avoiding internal leakage under high pressures. In [28], for instance, friction is intentionally added to an electric-actuated haptic device through a physical damper in order to increase the Z-width. Other factors, such as the sampling time and velocity filtering, have also been analyzed [15].

The following analysis is based on a linearized model of the HyQ leg. We linearized the rigid body dynamics and also the hydraulic actuator dynamics. The control system consists of a velocity compensation loop together with a PI controller [16] for the inner loop, and an outer Cartesian impedance PD controllers represented by the virtual elements shown in Fig. 2(a). Keeping the hip impedance constant ($K_{hip} = 70$ Nm/rad and $B_{hip} = 3$ Nms/rad), we vary the virtual leg stiffness from 1 up to 20000 N/m and the damping from 1 up to 1600 Ns/m, checking the passivity for every possible combination within this range. The nominal sampling time is $T_s = 0.001$ s and the inner PI torque controllers for both joints are identical and defined as:

$$C = K_{PI}\frac{0.03838\,(z - 0.9953)}{z - 1} \quad (2)$$

Changes on the gain K_{PI} of the *knee* PI torque controller has the most prominent impact on stability and passivity of the virtual leg. We have not investigated the effects of varying the location of the controller zero. Increasing K_{PI} by a factor of 2 reduced the passivity region to a maximum damping of $B = 440$ Ns/m (Fig. 3(a)), while decreasing it by a factor of 2 enlarged the passivity regions to cover

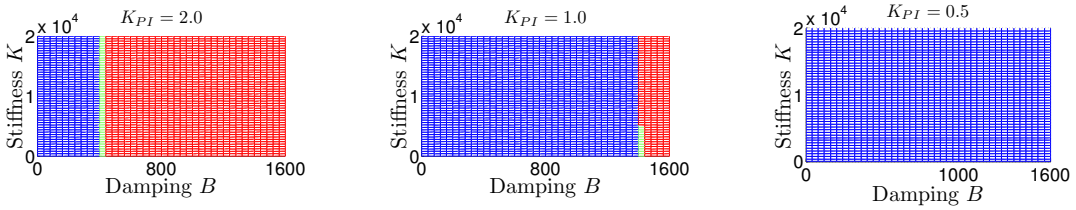

(a) (b) (c)

Fig. 3. Z-width (blue area) for the HyQ leg considering different K_{PI} gains for the knee PI torque controller: (a): $K_{PI} = 2$; (b): $K_{PI} = 1$; (c): $K_{PI} = 0.5$. The red area represents the *unstable* (and thus *non-passive*) range of impedances (with K expressed in N/m and B in Ns/m), the blue area the *passive* combinations of stiffness and damping, and the small green one where the system is *stable but not passive*. As we see, the higher the torque controller gain K_{PI} the smaller the Z-width.

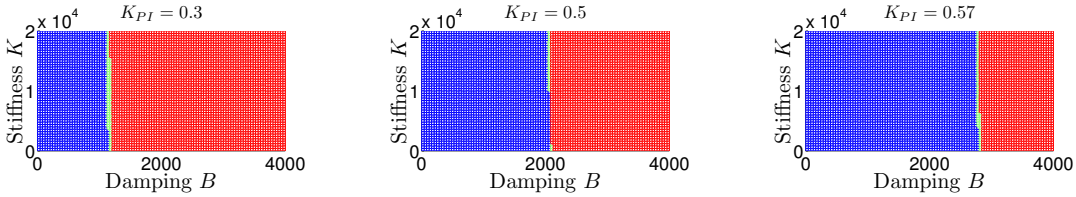

(a) 50 Hz (b) 150 Hz (c) 250 Hz

Fig. 4. Z-width for the HyQ leg with different valve bandwidths: (a): 50 Hz; (b): 150 Hz; (c): 250 Hz. The K_{PI} gain was adjusted to give the same closed-loop torque bandwidth of about 40 Hz with all the valves. Again, the red area represents the *unstable* range of impedances (with K expressed in N/m and B in Ns/m), the blue area the *passive* impedances, and the small green region the *stable, but not passive* combinations of stiffness and damping. As we can see, faster valves are able to increase the stable range of virtual impedances for a given closed-loop torque bandwidth.

all the chosen range of values for the virtual parameters (Fig. 3(c)) We obtained the passivity results shown in Fig. 3, using the criteria described at the beginning of Sec. III. Essentially, they show for which combination of stiffness and damping the system matrix $Y(z) + Y^*(Z)$ has a negative eigenvalue and/or $Y(z)$ is not stable, and thus not passive. The red areas represent those combinations where $Y(z)$ is *unstable* (i.e. where it has a pole outside the unit circle). The blue regions show where the system is *passive* (i.e. where all the eigenvalues of the matrix $Y(z) + Y^*(Z)$ are non-negative and $Y(z)$ is stable). Finally, the tiny green area depicts where $Y(z)$ is *stable but not passive* (i.e. where at least one eigenvalue of the matrix $Y(z)+Y^*(Z)$ is negative but $Y(z)$ still has all the poles inside the unit circle).

These results we show in Fig. 3 suggest that *the higher the torque loop gains, the smaller the range of impedances that can be passively rendered.* Although the system stability might benefit when using a low-gain torque controller, to intentionally reduce the torque controller performance may significantly restrict the compliant behavior of the robot, as we further discuss in Sec. IV-A. Therefore, in case a robot needs to enlarge its Z-width, to reduce the torque gains is not the best approach. In this case, an alternative is to change the actuator bandwidth. For valve-controlled hydraulic systems, as HyQ, it means to select a faster valve.

To assess the influence of the actuator dynamics in the Z-width, we selected three different valve bandwidths that are commonly available [29]: 50, 150, and 250 Hz. We used these values for computing a second-order transfer function for the valve dynamics which, together with the pressure dynamics, create the fourth-order [30] *Hydraulic dynamics* block shown in Fig. 1. For all these valve dynamics, we tunned the K_{PI} gain to give always the same closed-loop torque bandwidth of about 40 Hz. Then, we employed the same passivity criteria used in Fig. 3 to determine the Z-width with these three different valves. The results displayed in Fig. 4 clearly suggest that, given a closed-loop torque bandwidth, *higher valve bandwidths produce larger stable ranges of virtual impedances*. In this new analysis, we increased the damping range (from $B = 1600$ to $B = 4000$ Ns/m) with respect to the previous results (Fig. 3) so that we could see the effects of different valve dynamics in the Z-width. The effect of changes in stiffness was not relevant in the stiffness range of interest (1 to 20000 N/m).

IV. Experimental Results

In this section, we experimentally assess the impacts of the closed-loop torque performance in the actively-compliant behavior of HyQ's leg. In addition, we compare the actively-compliant HyQ leg with the specially-made passively-compliant version of the same leg (Fig. 2(b)).

A. Torque control performance influence

The compliance controller of HyQ uses a cascade control architecture (Fig. 1). In this arrangement, the inner torque loop performance influences both the passivity and stability as well as the performance of the outer compliance loop.

In Sec. III-A we showed that the performance of the inner torque loop affects the passivity of the outer loop. In general, the higher the torque controller gains the smaller the range of passive stiffness and damping (Z-width) that

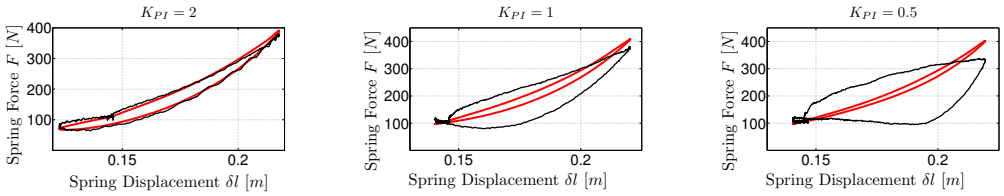

(a) (b) (c)

Fig. 5. Emulation of a virtual exponential spring-damper with different K_{PI} gains for the force controller: (a) $K_{PI} = 2$; (b) $K_{PI} = 1$; and (c) $K_{PI} = 0.5$. The leg was placed on the ground and pushed down by hand. The desired virtual leg reaction force profile is depicted in red, while the real behavior presented by the leg is shown in black.

can be employed in the outer loop. On the other hand, in this section we also demonstrate experimentally that although the system stability might benefit from using a low-gain torque controller, to intentionally reduce the inner torque controller performance can significantly restrict the apparent compliant behavior of the robot.

To asses the influence of the torque control performance on the compliant behavior of the robot, we used an exponential spring stiffness with a linear damping ($F = 17\, e^{10\,\delta l} + 50\,\dot{l}$). We put the leg on the ground and then manually pushed it down, compressing the virtual spring-damper, to verify the force reaction characteristics of the emulated compliant system. Figure 5(a) shows the tracking of the desired compliant behavior with $K_{PI} = 2$. Figure 5(b) and 5(c) demonstrate how the capability of the mimicking virtual compliant behaviors is strongly limited when the torque controller gains are reduced to $K_{PI} = 1$ and $K_{PI} = 0.5$ respectively. These results clearly demonstrate that, although a reduction in the torque performance might increase the stability ranges of the actively-compliant system, it can seriously hamper the compliant behavior of the robot.

B. Comparison with a real spring

As discussed previously, active compliance has been so far employed essentially in low-velocities tasks, such as assembly systems. The practical reason for that was the poor closed-loop torque bandwidth reached by such manipulators and also the weakness of mechanical parts such as gear boxes, which cannot tolerate high impact forces.

To experimentally assess the active compliance controller performance and stability for high-frequency perturbations, we dropped the actively-compliant leg from a height of 25 cm on a force plate, where we measured the ground reaction forces. Then, we removed the knee actuator (a hydraulic cylinder) which was emulating the virtual elements, and we physically added a spring-damper onto the leg as shown in Fig. 2(b), repeating the same experiment. The leg weight was not relevantly affected with this change. Furthermore, to be consistent with the physical spring assembly (Fig. 2(b)), for this experiment we moved the attachment point of the virtual spring (Fig. 2(a)) 6 cm away from the foot tip along the lower link axis so that both real and virtual springs were attached to the same point. The virtual stiffness ($K = 5250\ N/m$), damping ($B = 10\ Ns/m$)), and spring length ($l = 0.3\ m$) were also set to match the physical counterpart.

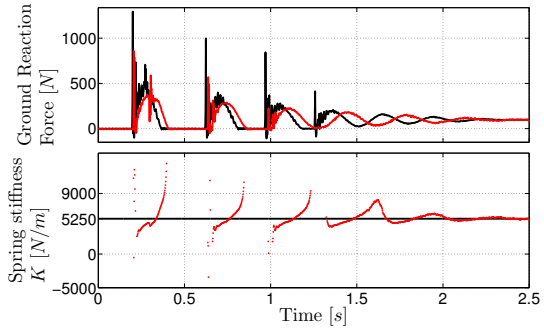

Fig. 6. Comparison of the leg dynamics when dropping it from 25 cm using two different compliance approaches: active compliance by using a virtual spring-damper (red line), and passive compliance by using a real spring-damper (black line). In the first plot, the vertical ground reaction forces show that both systems bounces with very similar dynamics, being the impact forces smaller for the actively-compliant leg. In the second plot, we show how the virtual leg tracks the desired stiffness of the real spring ($K = 5250\ N/m$) during stance phase.

The impact forces, measured by a force plate, and leg dynamics can be compared in the first plot of Fig. 6. As we can notice, the emulated spring-damper was able to qualitatively mimic the passive leg system. Small differences in the stance period suggest that the virtual spring (red line) had a smaller average stiffness value than the real spring (black line), creating then a longer stance phase. As we can see in the second plot, during stance phase the virtual stiffness is not constant, but it varies from about $K = 3500\ N/m$ to $K = 8000\ N/m$. This imprecise stiffness tracking, together with a possible non-ideal behavior of the real spring, can justify the slightly different dynamical behavior. Moreover, the real spring (black line) has a higher impact force (around 1300 N) than the virtual spring (about 800 N). This is a surprising result, since we expected that factors such as actuator dynamics and sampling would delay the virtual spring reaction, thus increasing the impact forces. The most probable reason for this smaller impact force of the virtual spring is the lower virtual stiffness value (around $K = 3500N/m$ against the real spring stiffness value of $K = 5250N/m$) at the moment of touch-down.

This example shows that a high-performance compliance controller can safely handle high-frequency disturbances inputs such as impact forces as well as emulate a desired compliance behavior.

V. Discussion

In this section, we discuss some of the results obtained in Sec. III-A and IV. In addition, we use the insights given by these stability and performance results to propose a procedure for systematically designing a compliance controller. However, before starting, we will briefly underline the *pros & cons* of both passive and active compliance. Such analysis is of fundamental importance for robot designers which have to decide between them, or a mix of both [31].

First of all, it should be clear that active compliance uses energy for producing the desired impedance behavior. This energy consumption can be a limiting factor for employing active compliance on robots that aim to be energy efficient. On the other hand, energy efficiency is one of the hallmarks of passive compliance. Components such as springs can store energy while being compressed (or extended). However, to enlarge the energy storage capabilities, usually small stiffness are used. This reduces the joint controllability, leading usually to poor position tracking and maybe, in the worst case, to dangerous situations [32]. Controllability is also a problem once the system (e.g. the arm) has been accelerated. It takes more time to stop it in case of an unexpected obstacle for example. For this reason and also due to design constraints, higher stiffness configurations are often preferred. In this case, the safety of the passive system is almost lost. Also, when the stored energy is suddenly released, it can result in high speed motions of the robot, and correspondingly in a high risk for humans in case of collision [33].

The application of passive compliance on a robot can be cheap. It can consist, for example, of a layer of rubber at the end-effector or a spring in series with it. However, more complex designs (e.g VSAs) can substantially increase the costs and complexity of passive compliance. Active compliance is usually more expensive to be employed than passive compliance. It commonly requires more hardware expenses, such additional force/torque sensors and extra data acquisition interfaces. In addition, if the actively-compliant robot intends to perform highly-dynamic tasks, high-performance (and normally high-priced) hardware is needed, such as high-bandwidth actuators and fast computers.

Although active compliance can be energy inefficient and sometimes expensive, its use is driven by a fundamental motivation: *versatility*. An actively-compliant robot can take advantage of any programmable type of impedance (e.g. exponential springs, nonlinear dampers, muscle-model-based springs, etc.) [12]. In this way, it is possible to considerably vary the dynamical robot's behavior with no physical changes on it. In hydraulically-actuated robots that use active compliance, it is possible to increase the valve efficiency at the price of a reduction in its bandwidth [29]. However, as we show in Fig. 4 and 5, low bandwidth valves and controllers can severely limit both the Z-width as well as the compliant behavior of the robot.

Based on the result shown in Fig. 5 and on the passivity analyses presented in Sec. III-A, we propose the following procedure to design a cascade compliance controller:

- The fist step should be the estimation of the range of impedances (Z-width) needed by the robot to satisfy all the requirements imposed by the tasks that it has to accomplish. For instance, a versatile robot as HyQ, which aims to perform many different tasks (e.g. walking, trotting, running, jumping), most likely requires a larger Z-width than a robot that is specific to a single application (e.g. walking or trotting).
- Once the Z-width is estimated, the inner torque controller should always be tuned to give the maximum stable closed-loop torque bandwidth which satisfies the limits imposed by the selected Z-width. This maximum closed-loop torque bandwidth will produce the best compliant performance for that Z-width (Fig. 5).
- Depending on the selected Z-width, this choice might limit the torque controller gains (Fig. 3) and consequently the compliant performance (Fig. 5). Therefore, in case the compliant performance does not satisfy the designer requirements, a faster actuator can be selected. As we show in Fig. 4, faster valves tend to produce larger stable ranges of impedance. Thus, higher gains/bandwidth can be achieved for the inner closed-loop torque controller.

This simple procedure might help robot controllers to find the most suitable trade-off between stability and performance. It gives some important practical insights to deal with instabilities in the compliance control loop. For instance, if some instability appears when increasing the damping in the legs, a reduction in the torque controller gains can solve this problem. Also, as described in [15], an increase in the sampling frequency or an averaging filtering in the velocity signal can also help in increasing the Z-width. Changes in the hardware might also be necessary for increasing the closed-loop torque bandwidth and/or the Z-width.

A limit in the torque performance will always exist, and it depends mainly on the load characteristics such as inertia and damping. Thus, depending on the load dynamics, it might be that in practice increasing the torque or actuator bandwidth does not necessarily improve the compliance tracking. In these cases, the only way to improve the compliance control performance is by changing the load characteristics. For instance, especially for low-inertia links, viscous friction could be intentionally added to the robot joint to improve the torque tracking at the price of energy loss.

VI. Conclusions and Future Work

We showed in this work that an actively-compliant robot with proper mechanical and control design can successfully emulate virtual passive elements under dynamic situations. For the first time, we experimentally demonstrate this capability by comparing the *actively-compliant* leg of HyQ with an identical *but passively-compliant* version of the same leg. The results confirm that active compliance is a suitable and interesting alternative to legged robots.

To ensure stable interactions with passive environments, we analyzed the range of achievable impedances that can be passively emulated at the contact point (Z-width). We

showed that, when a cascade compliance control architecture is used, the Z-width is strongly affected by the performance of the nested loop. In addition, we demonstrated that faster actuator bandwidths can increase the stable area of virtual impedances and produce better compliant performances. We used the results obtained to develop a simple procedure to design cascade compliance controllers.

Last but not least, having such torque-controlled machines will lead to a better understanding of how to build future robots, which might be more application specific and make use of passive elements to gain energy efficiency. The suitability of a passive element is easily tested by using virtual elements. For instance, if for a given set of applications it is found out that certain mimicked impedance characteristic is always appropriate, then the respective virtual element could be replaced by its real counterpart, leading to a mix of passive and active compliance.

Future work includes the analytical proof of the conjectures we propose about the influence of the actuator dynamics and torque controller gains in the Z-width; a systematic analysis of the required range of impedances for performing different tasks in different terrains; and also a gain scheduling scheme which can adjust the torque gains according to the impedance employed to ensure the leg is always passive.

APPENDIX - VIDEO CONTENTS

The video shows experiments with a single HyQ leg: (1) Drop test with real spring and virtual springs in real time; (2) Drop test in slow motion.

ACKNOWLEDGEMENTS

This research has been funded by the Fondazione Istituto Italiano di Tecnologia. Jonas Buchi is supported by a SNSF professorship.

REFERENCES

[1] M. T. Mason, "Compliance and force control for computer controlled manipulators," *Systems, Man and Cybernetics, IEEE Transactions on*, vol. 11, no. 6, pp. 418 –432, june 1981.

[2] D. E. Whitney, "Historical perspective and state of the art in robot force control," in *Robotics and Automation. Proceedings. 1985 IEEE International Conference on*, vol. 2, mar 1985, pp. 262 – 268.

[3] N. Hogan, "Impedance control: An approach to manipulation: Part II – Implementation," *ASME, Transactions, Journal of Dynamic Systems, Measurement, and Control*, vol. 107, pp. 8–16, 1985.

[4] O. Khatib, "A unified approach for motion and force control of robot manipulators: The operational space formulation," *Robotics and Automation, IEEE Journal of*, vol. 3, no. 1, pp. 43–53, 1987.

[5] J. Pratt, C. Chew, A. Torres, P. Dilworth, and G. Pratt, "Virtual model control: An intuitive approach for bipedal locomotion," *The International Journal of Robotics Research*, vol. 20, no. 2, pp. 129–143, 2001.

[6] W. P. Seering, "Understanding bandwidth limitations in robot force control," in *In Proceedings of the IEEE Conference on Robotics and Automation*, 1987, pp. 904–909.

[7] C. Klein and R. Briggs, "Use of active compliance in the control of legged vehicles," *IEEE Trans SMC*, vol. 10, no. 7, pp. 393–400, 1980.

[8] G. Pratt and M. Williamson, "Series elastic actuators," in *IEEE International Conference on Intelligent Robots and Systems (IROS)*, 1995.

[9] M. Grebenstein, A. Albu-Schaffer, T. Bahls, M. Chalon, O. Eiberger, W. Friedl, R. Gruber, S. Haddadin, U. Hagn, R. Haslinger, H. Hoppner, S. Jorg, M. Nickl, A. Nothhelfer, F. Petit, J. Reill, N. Seitz, T. Wimbock, S. Wolf, T. Wusthoff, and G. Hirzinger, "The dlr hand arm system," in *Robotics and Automation (ICRA), 2011 IEEE International Conference on*, may 2011, pp. 3175 –3182.

[10] N. G. Tsagarakis, I. Sardellitti, and D. G. Caldwell, "A new variable stiffness actuator (compact-vsa): Design and modelling," in *Intelligent Robots and Systems (IROS), 2011 IEEE/RSJ International Conference on*, sept. 2011, pp. 378 –383.

[11] A. Stienen, E. Hekman, H. ter Braak, A. Aalsma, F. van der Helm, and H. van der Kooij, "Design of a rotational hydroelastic actuator for a powered exoskeleton for upper limb rehabilitation," *Biomedical Engineering, IEEE Transactions on*, vol. 57, no. 3, pp. 728 –735, march 2010.

[12] T. Boaventura, C. Semini, J. Buchli, M. Frigerio, M. Focchi, and D. G. Caldwell, "Dynamic torque control of a hydraulic quadruped robot," in *IEEE International Conference in Robotics and Automation*, 2012, pp. 1889–1894.

[13] A. De Luca, A. Albu-Schaffer, S. Haddadin, and G. Hirzinger, "Collision detection and safe reaction with the dlr-iii lightweight manipulator arm," in *Intelligent Robots and Systems, 2006 IEEE/RSJ International Conference on*, Oct., pp. 1623–1630.

[14] J. E. Colgate and G. G. Schenkel, "Passivity of a class of sampled-data systems: Application to haptic interfaces," *Journal of Robotic Systems*, vol. 14, no. 1, pp. 37–47, 1997.

[15] F. Janabi-Sharifi, V. Hayward, and C.-S. Chen, "Discrete-time adaptive windowing for velocity estimation," *Control Systems Technology, IEEE Transactions on*, vol. 8, no. 6, pp. 1003 –1009, nov 2000.

[16] T. Boaventura, M. Focchi, M. Frigerio, J. Buchli, C. Semini, G. A. Medrano-Cerda, and D. G. Caldwell, "On the role of load motion compensation in high-performance force control," in *IEEE/RSJ International Conference on Intelligent Robots and Systems*, 2012.

[17] C. Semini, N. G. Tsagarakis, E. Guglielmino, M. Focchi, F. Cannella, and D. G. Caldwell, "Design of HyQ - a hydraulically and electrically actuated quadruped robot," *IMechE Part I: J. of Systems and Control Engineering*, vol. 225, no. 6, pp. 831–849, 2011.

[18] J. E. Colgate and J. M. Brown, "Factors affecting the z-width of a haptic display," in *IEEE International Conference on Robotics and Automation*, 1994, pp. 3205–3210.

[19] D. Hoyt and R. Taylor, "Gait and the energetics of locomotion in horses," *Nature*, vol. 292, pp. 239–240, 1981.

[20] M. Focchi, T. Boaventura, C. Semini, M. Frigerio, J. Buchli, and D. G. Caldwell, "Torque-control based compliant actuation of a quadruped robot," in *Proc. of the 12th IEEE Int. Workshop on Advanced Motion Control (AMC)*, 2012.

[21] R. Blickhan, "The spring-mass model for running and hopping," *J. Biomechanics*, vol. 22, no. 11–12, pp. 1217–1227, 1989.

[22] H. Geyer, A. Seyfarth, and R. Blickhan, "Spring-mass running: simple approximate solution and application to gait stability," *J. Theor. Biol.*, vol. 232, no. 3, pp. 315–328, 2004.

[23] E. Colgate and N. Hogan, "An analysis of contact instability in terms of passive physical equivalents," in *IEEE International Conference on Robotics and Automation*, 1989, pp. 404–409 vol.1.

[24] E. Fasse, "Stability robustness of impedance controlled manipulators coupled to passive environments," Master's thesis, MIT, Dept of Mech. Eng, June 1987.

[25] T. R. Kurfess, *Robotics and Automation Handbook*. CRC Press, 2004.

[26] B. D. O. Anderson and S. Vongpanitlerd, *Network Analysis and Synthesis – A Modern Systems Theory Approach*. Englewood Cliffs, NJ: Prentice-Hall, 1973, p. 548.

[27] J. E. Colgate, "Coupled stability of multiport systems – theory and experiments," *Transactions of ASME, Journal of Dynamic Systems, Measurement , and Control*, vol. 116, pp. 419–428, 1994.

[28] D. Weir, J. Colgate, and M. Peshkin, "Measuring and increasing z-width with active electrical damping," in *Symp. Haptic Interfaces for Virtual Environment and Teleoperator Systems*, 2008, pp. 169 –175.

[29] MOOG Inc., *Data Sheet of E024 Series Microvalve with Energy Efficient Low Flow Pilot Stage*, 2012.

[30] M. Jelali and A. Kroll, *Hydraulic Servo-systems. Modelling, Identification and Control*. Springer, 2003.

[31] W. Wang, R. N. Loh, and E. Y. Gu, "Passive compliance versus active compliance in robot-based automated assembly systems," *Industrial Robot: An International Journal*, vol. 25, Iss: 1, pp. 48–57, 1998.

[32] J. W. Hurst, D. Hobbelen, and A. Rizzi, "Series elastic actuation: Potential and pitfalls," in *Proceedings of the International Conference on Climbing and Walking Robots (CLAWAR)*, September 2004.

[33] B. Vanderborght, *Dynamic Stabilisation of the Biped Lucy Powered by Actuators with Controllable Stiffness*, ser. Springer Tracts in Advanced Robotics. Springer, 2010.